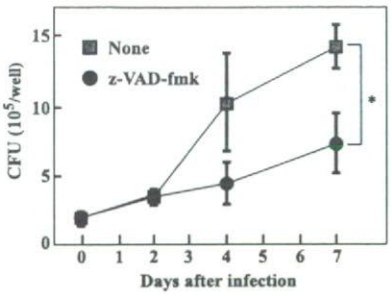

FIG. 1. Kinetics of intracellular growth of H37Rv in RAW 264 cells treated with or without z-VAD-fmk. RAW 264 cells were infected with H37Rv at an MOI of 5 and cultured in the presence or absence of 40 μM z-VAD-fmk. Cells were lysed at the indicated days, and the number of viable bacteria was determined by a CFU assay. Data represent the means ± standard deviations for triplicate assays and are representative of three independent experiments. *, $P < 0.05$.

growth was observed in z-VAD-fmk-treated macrophages for 2 days after infection. However, the growth rate was suppressed afterwards. To rule out the possibility that the growth inhibition is due to the direct action of z-VAD-fmk on H37Rv, we incubated H37Rv (5×10^5 CFU) in Middlebrook 7H9 broth including albumin, dextrose, and catalase for 7 days in the presence or absence of z-VAD-fmk and recovered 1.52×10^7 CFU or 1.56×10^7 CFU of H37Rv from the culture, respectively. A similar result was observed when H37Rv was cultured in the cell culture medium (data not shown). The results showed that z-VAD-fmk by itself did not influence bacterial growth and raised the possibility that some initiator and/or effector caspases were involved in facilitating the intracellular survival of H37Rv. Several studies clearly showed that caspase-8 and caspase-9 (initiator caspases) and caspase-3 (an effector caspase) are activated after *M. tuberculosis* infection and cause cell death in infected macrophages (22). Thus, we speculated that these caspases might have some activity influencing the fate of intracellular bacteria. To make this point clear, we examined whether these caspases were activated after infection with H37Rv and whether z-VAD-fmk inhibited the activation. As shown in Fig. 2, a significant level of caspase-8 activation was observed 1 day after infection and the activity decreased back to the control level by 2 days. The activities of caspase-3/7 and caspase-9 were increased on day 2 about four- and twofold, respectively. These caspase activities were at the control level on day 5, indicating that H37Rv induced activation of caspases to some extent. On the other hand, H37Rv-induced activations of these caspases were mostly inhibited in the presence of z-VAD-fmk and were not affected by z-FA-fmk (an inactive caspase inhibitor analogue). Since growth inhibition of the intracellular bacteria was detected in z-VAD-fmk-treated cells later than 2 days after infection, the results suggest that caspases may play a role in the intracellular survival of virulent *M. tuberculosis*.

z-VAD-fmk treatment causes necrosis of infected RAW 264 cells. To find the reason z-VAD-fmk treatment inhibited bacterial growth, on day 3 of infection, infected cells in the presence or absence of z-VAD-fmk were examined under an electron microscope. We did not detect any morphological change between normal cells (Fig. 3A) and cells treated only with z-VAD-fmk for 3 days (Fig. 3B). However, we found that infection of RAW 264 cells with H37Rv influenced cell morphology. Among the infected cells, 42% of the cells maintained their cellular structures (Fig. 3C and D) and 26% showed apoptotic structural changes (Fig. 3E). The remaining 32% of the cells displayed morphological changes characteristic of necrosis (Fig. 3F). The treatment with z-VAD-fmk provoked

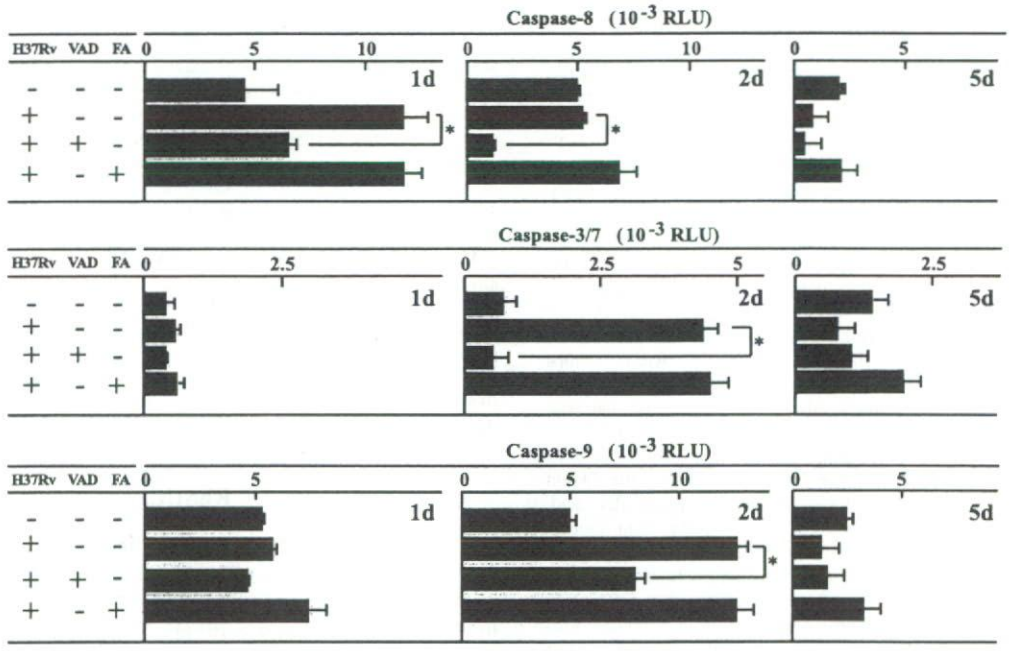

FIG. 2. Caspase activities after infection with H37Rv. RAW 264 cells were infected with H37Rv, and caspase activities were measured at 1, 2, and 5 days after infection by a Caspase-Glo assay. VAD, z-VAD-fmk; FA, z-FA-fmk; RLU, relative light units. Data represent the means ± standard deviations for triplicate assays and are representative of three independent experiments. *, $P < 0.05$.

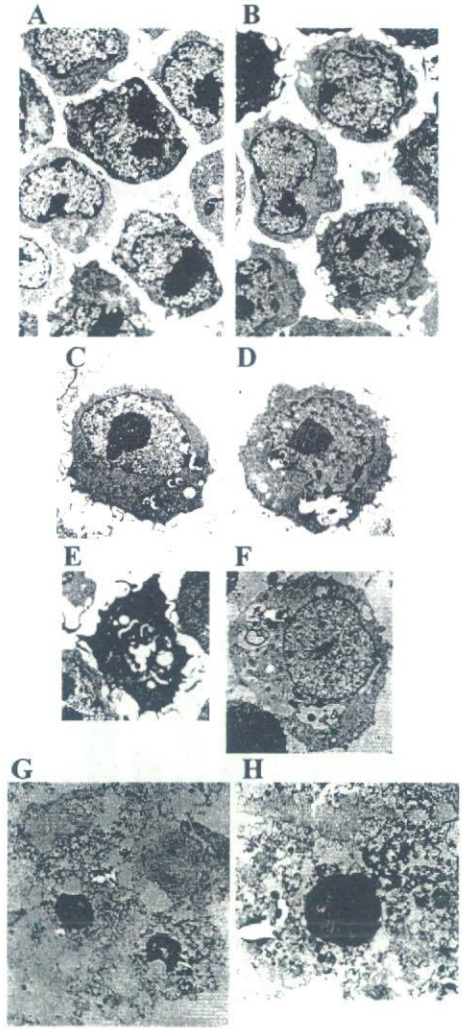

FIG. 3. Effect of z-VAD-fmk on morphologies of infected cells. RAW 264 cells infected with H37Rv were cultured for 3 days in the absence (C to F) or presence (G, H) of z-VAD-fmk. Cells were fixed, and morphologies were observed under an electron microscope. (E) A representative apoptotic cell. (F) A cell showing necrotic damage. (C and D) Infected cells which maintained normal cell morphologies. (A and B) Nontreated cells (A) and cells treated only with z-VAD-fmk (B). Micrographs were taken at magnifications of ×5,000 (A to F and H) and ×3,000 (G).

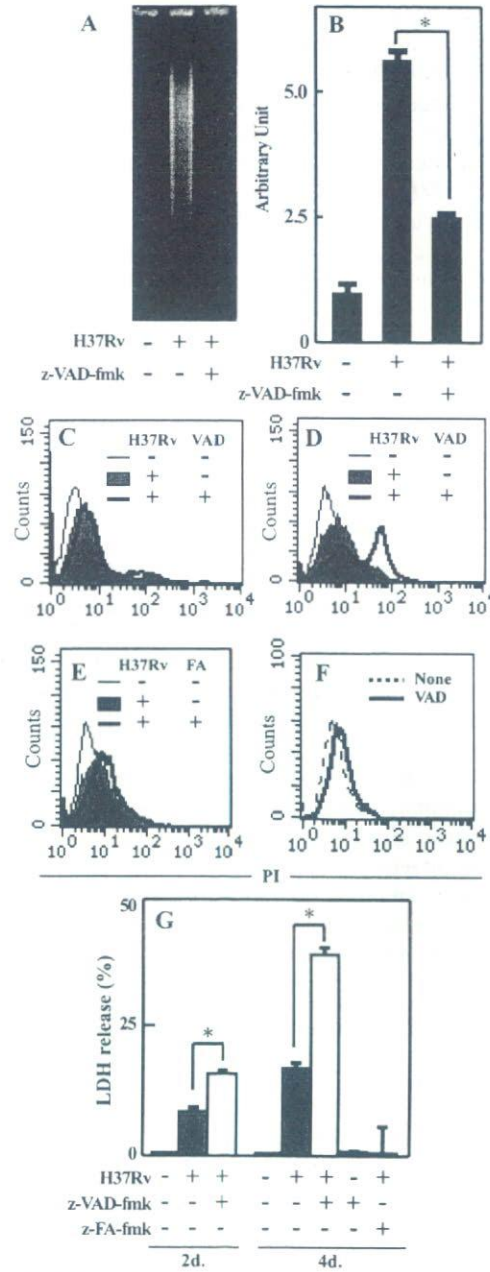

FIG. 4. Inhibition of apoptosis and induction of necrosis by z-VAD-fmk treatment. RAW 264 cells were infected with H37Rv and cultured for 2 days. Cells were lysed, and the DNA ladder and oligonucleosomes were detected by agarose gel electrophoresis (A) and quantified by an enzyme-linked immunosorbent assay (B), respectively. Two days (C) and 4 days (D, E) after infection, the cells were stained with PI and fluorescence intensity was measured. VAD, z-VAD-fmk; FA, z-FA-fmk. (F) Fluorescence intensity of the cells treated only with z-VAD-fmk for 4 days. (G) Culture supernatants were collected 2 and 4 days after infection, and LDH activity was assayed. Data represent the means ± standard deviations for triplicate assays and are representative of three independent experiments. *, $P < 0.05$.

much severe damage in the infected cells. As shown in Fig. 3G and H, the caspase inhibitor caused necrotic morphological changes in as many as 95% of the infected cells. These results raised the possibility that some caspases contribute to inhibition of necrosis of infected cells in conventional infection in vitro. To confirm that the morphological changes resulted from apoptosis or necrosis of the infected cells, we investigated a generation of oligonucleosomes and assessed the membrane integrity of the infected cells by measuring the population of PI-stained cells and LDH release into the culture medium. As shown in Fig. 4A, an oligonucleosomal DNA ladder was observed in RAW 264 cells infected with H37Rv but not in uninfected cells. Treatment with z-VAD-fmk clearly inhibited the cleavage of DNA. To analyze the DNA fragmentation quantitatively, the cell lysates were subjected to a sandwich enzyme-linked immunosorbent assay specific for oligonucleosomes. The number of oligonucleosomes in H37Rv-infected cells was about 5 times as high as that in the uninfected cells, but z-VAD-fmk significantly inhibited the generation of oligo-

nucleosomes (Fig. 4B). These results clearly indicated that z-VAD-fmk inhibited the apoptotic process induced by infection with H37Rv. On the other hand, though the infected cells were not stained with PI for 2 days after infection, irrespective of z-VAD-fmk treatment, the fluorescence intensities in both groups increased at day 4 postinfection (Fig. 4C and D). In the absence of z-VAD-fmk treatment, cells were stained intermediately with PI and could be divided into two populations based on fluorescence intensity. Since the number of cells expressing the brighter fluorescence reached 32.2% of the total number of cells and 32% of the infected cells exhibited necrotic morphologies (Fig. 3), it seemed that the cells stained highly with PI represented the cells undergoing necrosis. On the other hand, most of the z-VAD-fmk-treated cells were stained strongly with PI 4 days after infection, while z-FA-fmk treatment did not increase the number of damaged cells in the population (Fig. 4E). PI-stained cells were never observed in noninfected cells treated with z-VAD-fmk alone (Fig. 4F). In addition, z-VAD-fmk treatment caused a lower but a significant level of LDH release from the infected cells 2 days after infection, and the release was dramatically enhanced on day 4. Again, there was no LDH release at all from the cells treated with z-VAD-fmk alone even after 4 days in the absence of *M. tuberculosis* infection (Fig. 4G). Furthermore, z-FA-fmk treatment did not induce LDH release from the infected cells. These results strongly suggested that H37Rv induced the activation of caspases, resulting in not only the induction of apoptosis but also the inhibition of necrosis of infected cells.

Involvement of ROS accumulation in z-VAD-fmk-induced necrosis of infected cells. Vercammen et al. have shown that L929 fibrosarcoma cells treated with z-VAD-fmk rapidly died from necrosis after treatment with TNF-α. Necrotic cell death was induced also by overexpression of cytokine response modifier A (CrmA), a serpin-like caspase inhibitor (12, 32). In these reports, they indicated that the necrosis was provoked by ROS that was generated by inhibition of caspases. Since H37Rv infection induced severe necrosis of infected cells when the cells were treated with a caspase inhibitor, we examined whether z-VAD-fmk treatment triggers ROS generation in H37Rv-infected cells by using DCFH-DA, a fluorescent detector of ROS. RAW 264 cells were infected with H37Rv for 2 days in the presence or absence of z-VAD-fmk and treated with DCFH-DA for 15 min. The fluorescence of DCFH emitted in cytoplasm after oxidization by ROS was measured by FACSCalibur. The fluorescence intensity of the infected cells was increased significantly by treatment with z-VAD-fmk (Fig. 5A). However, enhancement of fluorescence was diminished by addition of BHA, a scavenger of ROS generated intracellularly, indicating that z-VAD-fmk treatment induced the generation of ROS in the infected cells (Fig. 5B). We further found that BHA treatment suppressed the z-VAD-fmk-induced necrosis of H37Rv-infected cells, because both the fluorescence intensity of the PI-stained cells and the LDH release from the cells were decreased markedly by BHA (Fig. 5C and D). In addition, though treatment with z-VAD-fmk inhibited the intracellular growth of H37Rv, the inhibitory activity was cancelled appreciably by treatment with BHA (Fig. 5E). Furthermore, our data showed that the low level of intracellular ROS that was generated by H37Rv alone did not affect the bacterial growth, because BHA treatment did not influence the

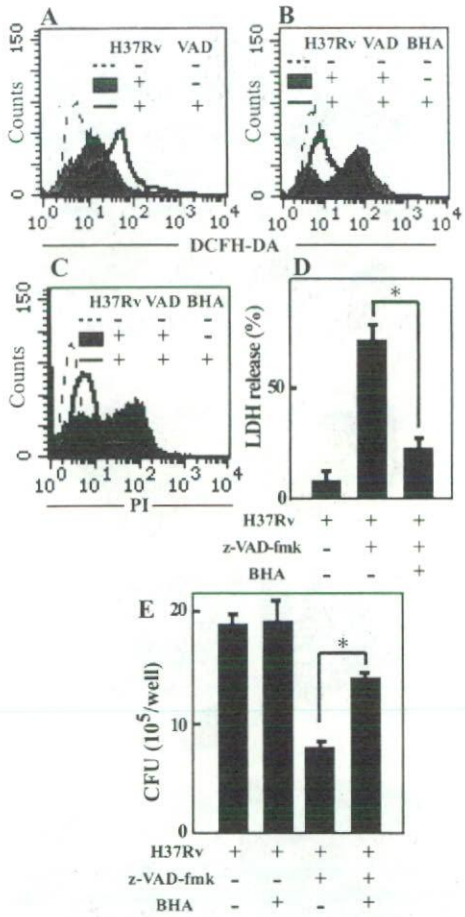

FIG. 5. Involvement of intracellular ROS accumulation in induction of necrosis and inhibition of intracellular bacterial growth. (A) RAW 264 cells were infected with H37Rv and cultured for 2 days in the presence or absence of z-VAD-fmk. Cells were treated with 5 μM DCFH-DA, and the fluorescence intensity of the oxidized DCFH was measured. (B) RAW 264 cells were infected and cultured for 2 days with or without z-VAD-fmk and an antioxidant reagent, BHA (25 μM). The cells were treated with DCFH-DA, and fluorescence intensity was measured. (C) Two days after infection, the cells were collected and cell permeability to PI was measured. (D) RAW 264 cells were infected and cultured for 4 days. The culture supernatant was collected, and the LDH activity was measured. (E) RAW 264 cells were infected and cultured for 7 days with or without z-VAD-fmk and BHA. The cells were lysed, and the number of intracellular bacteria was determined. Data represent the means ± standard deviations for triplicate assays and are representative of three independent experiments. *, $P < 0.05$.

intracellular bacterial number. These results indicated that inhibition of caspase activities by z-VAD-fmk induced the high level of ROS generation in the cytoplasm of H37Rv-infected cells. The intracellular ROS appeared to contribute to the induction of necrosis and the arrest of intracellular growth of H37Rv.

Critical involvement of caspase-9 in the inhibition of necrosis. Because z-VAD-fmk is a broad-spectrum caspase inhibitor capable of inhibiting the activity of caspases in general (23, 27), we next tried to identify the particular caspase involved in the inhibition of necrosis of infected cells. To address this point, we employed specific inhibitors for caspase-1, caspase-2,

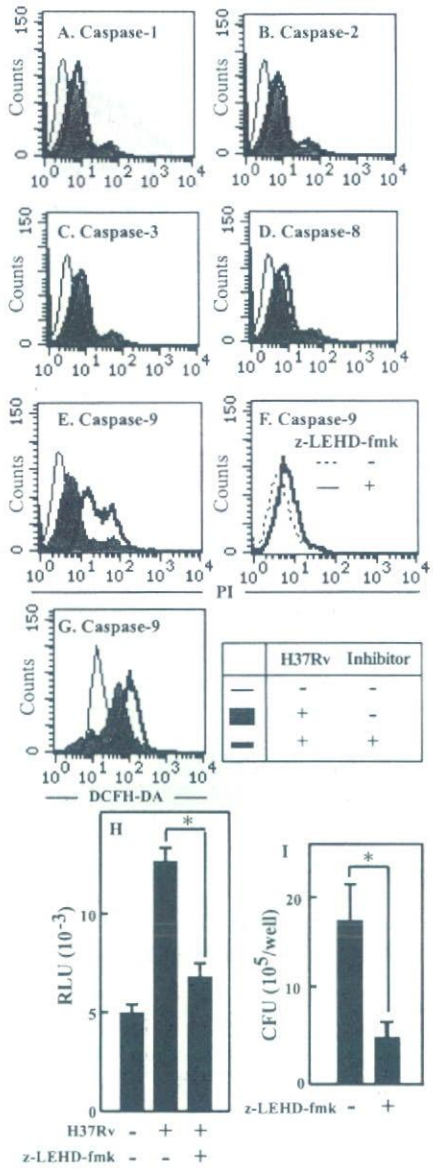

FIG. 6. Effects of inhibitors (120 μM) for caspase-1, -2, -3, -8, and -9 on induction of necrosis and intracellular bacterial growth. RAW 264 cells were infected with H37Rv and incubated with or without inhibitors specific for caspase-1 (A), caspase-2 (B), caspase-3 (C), caspase-8 (D), or caspase-9 (E). After 3 days of cultivation, membrane permeability was assessed by PI staining. (F) The caspase-9 inhibitor does not affect membrane permeability. (G) RAW 264 cells were infected and cultured for 2 days with or without z-LEHD-fmk, and the cells were stained with DCFH-DA and measured for fluorescence derived from oxidized DCFH. (H) RAW 264 cells were infected and cultured for 2 days with or without z-LEHD-fmk. Caspase-9 activity was measured by a Caspase-Glo assay. (I) Seven days after infection and cultivation with z-LEHD-fmk, the number of intracellular bacteria was determined by a CFU assay. Data represent the means ± standard deviations for triplicate assays and are representative of three independent experiments. *, $P < 0.05$. RLU, relative light units.

caspase-3, caspase-8, and caspase-9 (10, 17, 31) instead of z-VAD-fmk and determined the effect of each inhibitor on necrosis of H37Rv-infected cells by measuring membrane permeability. Although inhibitors of caspase-1, caspase-2, caspase-3, and caspase-8 did not change the PI-staining pattern

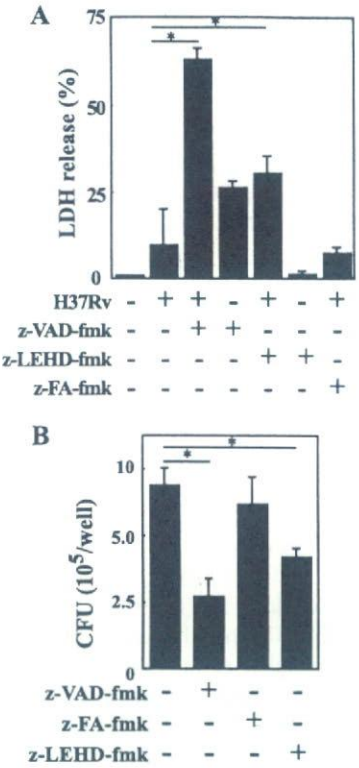

FIG. 7. Effects of caspase inhibitors on necrosis of H37Rv-infected macrophages and intracellular growth of bacteria. Peritoneal exudate macrophages were infected with H37Rv at an MOI of 5 in the presence or absence of caspase inhibitors. (A) Culture supernatants were collected 1 day after infection, and LDH activity was assayed. (B) Cells were infected with H37Rv and incubated for 7 days in the presence or absence of caspase inhibitors. The number of intracellular bacteria was determined by a CFU assay. Data represent the means ± standard deviations for triplicate assays and are representative of three independent experiments. *, $P < 0.05$.

of the infected cells (Fig. 6A to D), only the caspase-9 inhibitor (z-LEHD-fmk) enhanced the fluorescence intensity (Fig. 6E). The inhibitor itself did not affect the membrane permeability (Fig. 6F). Furthermore, we found that z-LEHD-fmk enhanced the fluorescence intensity of oxidized DCFH in the infected cells (Fig. 6G) and inhibited the intracellular growth of H37Rv (Fig. 6I). Activation of caspase-9 in H37Rv-infected cells was significantly abolished in the presence of z-LEHD-fmk (Fig. 6H). These results suggested that caspase-9 which was activated by H37Rv infection contributed to the inhibition of necrosis through regulation of intracellular ROS generation.

Detection of caspase-9-dependent inhibition of bacterial growth and necrosis in peritoneal macrophages. To analyze whether caspase-9-dependent inhibition of necrosis is a general intracellular event after H37Rv infection, we infected thioglycolate-induced peritoneal macrophages with H37Rv in the presence or absence of z-VAD-fmk or z-LEHD-fmk and measured LDH release. Similar to H37Rv infection in RAW 264 cells, H37Rv induced only a low level of LDH release from the infected macrophages and z-FA-fmk did not augment the response (Fig. 7A). However, treatment with z-VAD-fmk and z-LEHD-fmk caused a high level of LDH release from the infected macrophages compared to treatment with caspase

inhibitor alone or H37Rv infection without treatment with these inhibitors (Fig. 7A). In addition, we found that treatment with z-VAD-fmk or z-LEHD-fmk significantly reduced the intracellular number of bacteria (Fig. 7B). These data are consistent with those obtained from RAW 264 cells, suggesting that caspase-9 generally contributes to inhibition of necrosis in macrophages after *M. tuberculosis* infection.

Difference between the abilities of H37Rv and H37Ra to induce necrosis and apoptosis and activate caspase-9. We next investigated the abilities of H37Rv and H37Ra in induction of apoptosis and necrosis and activation of caspase in RAW 264 cells to determine whether H37Rv-induced responses are associated with the virulence of *M. tuberculosis*. Two days after infection, H37Rv induced LDH release from the infected cells while such a level of LDH release was not detected in the supernatant of cells infected with H37Ra (Fig. 8A). In contrast, a significant number of oligonucleosomes was detected in the lysate of H37Ra-infected cells, which was higher than that in the H37Rv-infected cells (Fig. 8B). In addition, we found that H37Ra induced a higher level of caspase-3/7 and caspase-8 activation than H37Rv. These results indicated that H37Rv but not H37Ra caused necrosis of RAW 264 cells and that H37Ra had a higher ability in induction of apoptosis than H37Rv. In this experimental model, as described formerly, H37Rv induced a high level of LDH release from the cells cultured in the presence of z-VAD-fmk, while H37Ra caused only a moderate level of LDH release (Fig. 8A). In contrast to the strong activities of caspase-9 and the active caspase-9 fragment in the lysate of H37Rv-infected cells (Fig. 8C and D), H37Ra could not induce such levels of caspase-9 activation. The amount of the active form of caspase-9 detected in H37Ra infection was smaller than that induced by H37Rv infection (Fig. 8C and D). It may be suggested that virulent *M. tuberculosis* has the ability to cause necrosis of the infected macrophages but, at the same time, is capable of activating caspase-9 in order to evade immediate necrotic cell death after infection in host cells where *M. tuberculosis* must reside for a longer period.

DISCUSSION

In the present study, we showed that H37Rv induced the activation of various caspases and that some of the infected cells underwent apoptosis 2 days after infection. Our initial presumption was, therefore, that the addition of the broad-spectrum caspase inhibitor z-VAD-fmk might simply block the apoptosis of RAW 264 cells infected with H37Rv and facilitate the bacterial growth inside. Indeed, generation of oligonucleosomes, which is a representative parameter for apoptosis, was significantly inhibited by the addition of z-VAD-fmk. To our surprise, however, the treatment instead caused necrosis in a very high proportion of the infected cells. These results strongly suggested that some caspases contribute to the inhibition of necrosis of RAW 264 cells induced by H37Rv infection. By using a panel of inhibitors specific for each caspase, we were able to find that caspase-9 is responsible for such an effect through inhibition of intracellular ROS generation. The less virulent strain H37Ra hardly induced caspase-9 activation, and necrosis of infected cells could not be observed even in the presence of z-VAD-fmk. It was suggested that caspase-9-de-

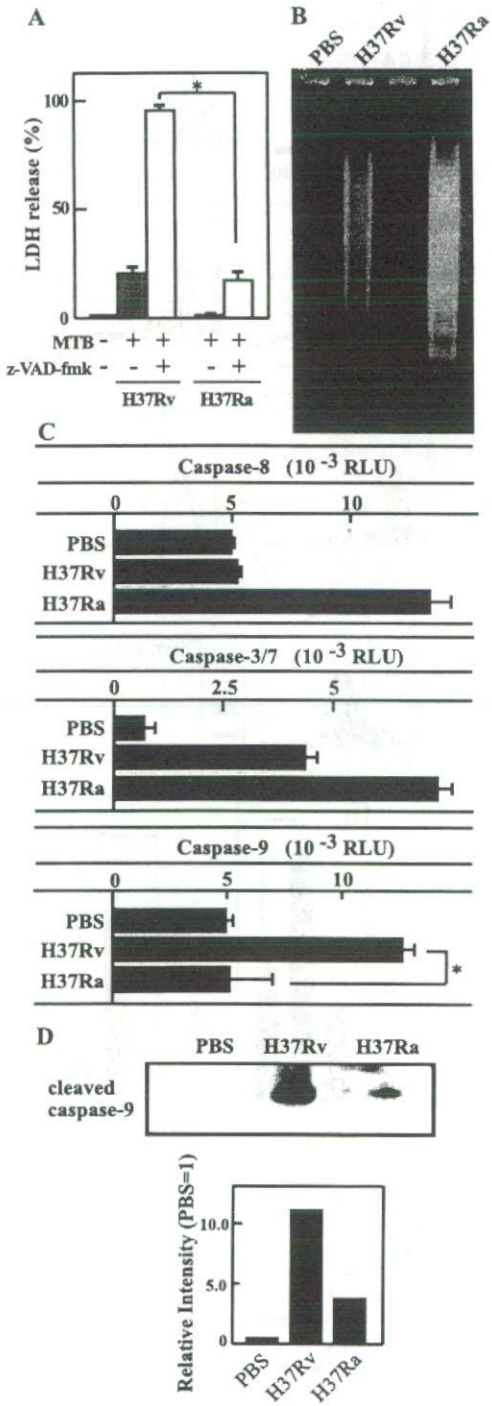

FIG. 8. Differences between the abilities of the *M. tuberculosis* H37Rv and H37Ra strains to induce apoptosis, necrosis, and caspase activation in RAW 264 cells. RAW 264 cells were infected with H37Rv or H37Ra at an MOI of 5 in the presence or absence of z-VAD-fmk. (A) The culture supernatant was collected 4 days later, and LDH activity was measured. Two days after cultivation, cells were lysed and the DNA ladder was detected by agarose gel electrophoresis (B) and caspase activities were measured by a Caspase-Glo assay (C). (D) The cell lysate was applied on a sodium dodecyl sulfate-polyacrylamide gel electrophoresis gel, and the amount of active form of caspase-9 was analyzed by Western blotting with caspase-9-specific antibody. The relative intensities of the bands are indicated in the lower graph. Data represent the means ± standard deviations for triplicate assays and are representative of three independent experiments. *, $P < 0.05$.

pendent inhibition of necrosis is related to the virulence of *M. tuberculosis*.

Based on our preliminary study, we selected concentrations of caspase inhibitors suitable for suppression of caspase activities. Schaible et al. used the caspase inhibitor z-VAD-fmk at the same concentration for their investigation (25). Although the appropriate concentration might be high, it might not be high, and it probably differs on the basis of experimental conditions. In the presence of a broad-spectrum caspase inhibitor or caspase-9-specific inhibitor, the growth of H37Rv was limited in RAW 264 cells that underwent necrosis. The current consensus is that apoptosis of macrophages results in the limitation of intracellular survival of *M. tuberculosis* but that necrosis does not affect the intracellular bacteria and helps *M. tuberculosis* in dissemination to other macrophages. Recent evidence further demonstrates that virulent *M. tuberculosis* possesses some inhibitory mechanisms of apoptosis that can be easily induced by less virulent strains (6, 15). In the present experiments, using RAW 264 cells, we observed that H37Ra induced a higher level of DNA fragmentation than H37Rv. In contrast, H37Rv infection caused a significant level of LDH release whereas H37Ra hardly induced LDH release during the initial period of infection. These results are consistent with observations published elsewhere (6, 15). In addition, we found that intracellular growth was inhibited in RAW 264 cells in which severe apoptosis was induced by treatment with actinomycin D (data not shown). As shown here, z-VAD-fmk and z-LEHD-fmk treatment caused severe necrosis of infected cells and the magnitude of necrosis was markedly different from that induced by H37Rv infection alone. It appears that induction of an excessive level of necrosis or apoptosis may eliminate the favorable niche for bacterial growth, resulting in the inhibition of bacterial multiplication in host cells. Our finding is not against the consensus, and we believe that this study could give insight into the role of caspase-9 in the fate of intracellular *M. tuberculosis*. Although the present data did not reveal whether necrosis of the infected macrophages affected bacterial replication in vivo, it has been reported that uncontrolled mycobacterial growth was observed in necrotic regions in the lungs of *sst1*^{s} mice and TNF-α or gamma interferon knockout mice (4, 8, 11, 19, 24). Because activation of the necrosis pathway may allow acceleration of bacterial growth and exacerbation of mycobacterial infection, the caspase-9-dependent necrosis inhibition that was presented in this study may be of additional importance in host defense against infection with virulent *M. tuberculosis*.

It has been shown that several kinds of caspase species contribute to inhibition of necrosis (18). Vercammen et al. have reported that TNF-α-stimulated L929 cells undergo necrosis when the cells are treated with a caspase inhibitor. They suggested that caspase-1 and caspase-3 might play a role in the inhibition of both ROS generation and necrosis (12, 31). On the other hand, other reports have shown that interaction of FasL and Fas induces necrosis if caspase-8 is inhibited (13, 17, 31). It is reported that caspase-8 inhibits necrosis by inhibition of binding of receptor-interacting protein to the death domain of the Fas receptor (13). In the present study, using *M. tuberculosis* infection in vitro, we found that caspase-9, but not caspase-1, -3, or -8, exerted a critical role in the inhibition of necrosis. Since there were differences in the requirements of particular caspases to inhibit necrosis of infected cells, it appeared that distinctive signal pathways were activated. One possible interpretation for the caspase-9-dependent inhibition of necrosis is that caspase-9 contributes to stabilization of the mitochondrial membrane and inhibition of ROS production from mitochondria. It has been shown that an excessive generation of ROS was induced from mitochondria in L929 cells after stimulation with TNF-α in the presence of an inhibitor for caspase-1 or caspase-3 (12, 31). Matsumura et al. have shown that a reduction of mitochondrial transmembrane potential ($\Delta\psi m$) was observed in JmF cells treated with FasL and z-VAD-fmk (17) and that pyrrolidine dithiocarbamate, a metallo chelator and antioxidant, efficiently inhibited FasL-induced necrosis. Our preliminary study also showed that z-VAD-fmk treatment caused a reduction of $\Delta\psi m$ in H37Rv-infected cells (data not shown). Since the intracellular concentration of ROS was increased when cells were infected with H37Rv in the presence of the caspase-9 inhibitor, caspase-9 might contribute to the inhibition of mitochondrial membrane damage. Further studies are needed to determine the precise mechanism.

It has been reported that various bacterial components are involved in apoptosis induction in cells infected with *M. tuberculosis*. There are several reports showing that 19-kDa lipoprotein and lipomannan derived from *M. tuberculosis* induced the apoptosis of macrophages or neutrophils (1, 5, 6, 9, 16). It was also reported that TNF-α was produced after infection with *M. tuberculosis* and caused apoptosis of macrophages (2, 22). On the other hand, other reports demonstrated that *M. tuberculosis* possesses an activity inhibiting apoptosis induction. Sly et al. showed that H37Rv had a weaker activity in induction of apoptosis than the attenuated H37Ra strain, and this was due to up-regulation of antiapoptotic gene expression in H37Rv-infected cells (28). Because the intracellular growth of H37Ra in RAW 264 cells was limited compared to that of H37Rv (data not shown), it is possible that activation of the inhibitory process facilitates the intracellular replication of H37Rv. On the other hand, H37Rv caused necrosis when infected cells were treated with the caspase-9 inhibitor. However, H37Ra hardly induced necrosis of cells treated with the inhibitor. Furthermore, we found that caspase-9 was not activated by infection with the attenuated H37Ra strain. Hsu et al. have shown that a mutant strain of H37Rv which is deficient for the *RD1* (region of difference 1) region is attenuated for virulence and necrosis-inducing abilities (14). In addition, Park et al. have shown that virulent clinical isolates of mycobacteria strongly induced necrosis of infected macrophages (20). Taken together, these results and our findings suggest that necrosis-inducing activity is associated with the virulence of *M. tuberculosis* and that caspase-9 activation is probably linked with some mycobacterial virulence determinant.

In conclusion, our present study clearly demonstrated that caspase-9 has a pivotal role in regulation of necrosis induced by infection with H37Rv. We are now trying to address how caspase-9 is activated and how the caspase inhibits necrosis of infected cells. In addition, because necrosis induction appears to be associated with the virulence of mycobacteria, further analysis on the bacterial factor responsible for caspase-9 induction may provide some novel insight for further understanding of host-*M. tuberculosis* interaction.

ACKNOWLEDGMENTS

This work was supported by a Grant-in-Aid for Scientific Research on Priority Areas (C) from the Ministry of Education, Science, Culture and Sports of Japan; by a Grant-in-Aid for Scientific Research (B and C) from The Japan Society for the Promotion of Science; and in part by a Grant-in-Aid for Scientific Research from the Ministry of Health, Labor and Welfare, Japan.

REFERENCES

1. **Alemán, M., P. Schierloh, S. S. de la Barrera, R. M. Musella, M. A Saab, M. Baldini, E. Abbate, and M. C. Sasiain.** 2004. *Mycobacterium tuberculosis* triggers apoptosis in peripheral neutrophils involving Toll-like receptor 2 and p38 mitogen protein kinase in tuberculosis patients. Infect. Immun. **72:**5150–5158.
2. **Balcewicz-Sablinska, M. K., J. Keane, H. Kornfeld, and H. G. Remold.** 1998. Pathogenic *Mycobacterium tuberculosis* evades apoptosis of host macrophages by release of TNF-R2, resulting in inactivation of TNF-α. J. Immunol. **161:**2636–2641.
3. **Bass, D. A., J. W. Parce, L. R. Dechatelet, P. Szejda, M. C. Seeds, and M. Thomas.** 1983. Flow cytometric studies of oxidative product formation by neutrophils: a graded response to membrane stimulation. J. Immunol. **130:**1910–1917.
4. **Bean, A. G. D., D. R. Roach, H. Briscoe, M. P. France, H. Korner, J. D. Sedgwick, and W. J. Britton.** 1999. Structural deficiencies in granuloma formation in TNF gene-targeted mice underlie the heightened susceptibility to aerosol *Mycobacterium tuberculosis* infection, which is not compensated for by lymphotoxin. J. Immunol. **162:**3504–3511.
5. **Ciaramella, A., A. Cavone, M. B. Santucci, S. K. Garg, N. Sanarico, M. Bocchino, D. Galati, A. Martino, G. Auricchio, M. D'Orazio, G. R. Stewart, O. Neyrolles, D. B. Young, V. Colizzi, and M. Fraziano.** 2004. Induction of apoptosis and release of interleukin-1β by cell wall-associated 19-kDa lipoprotein during the course of mycobacterial infection. J. Infect. Dis. **190:**1167–1176.
6. **Ciaramella, A., A. Martino, R. Cicconi, V. Colizzi, and M. Fraziano.** 2000. Mycobacterial 19-kDa lipoprotein mediates *Mycobacterium tuberculosis*-induced apoptosis in monocytes/macrophages at early stages of infection. Cell Death Differ. **7:**1270–1272.
7. **Clark-Curtiss, J. E., and S. E. Haydel.** 2003. Molecular genetics of *Mycobacterium tuberculosis* pathogenesis. Annu. Rev. Microbiol. **57:**517–549.
8. **Cooper, A. M., D. K. Dalton, T. A. Stewart, J. P. Griffin, D. G. Russell, and I. M. Orme.** 1993. Disseminated tuberculosis in interferon γ gene-disrupted mice. J. Exp. Med. **178:**2243–2247.
9. **Dao, D. N., L. Kremer, Y. Guérardel, A. Molano, W. R. Jacobs, Jr., S. A. Porcelli, and V. Briken.** 2004. *Mycobacterium tuberculosis* lipomannan induces apoptosis and interleukin-12 production in macrophages. Infect. Immun. **72:**2067–2074.
10. **Faraco, P. R., E. C. Ledgerwood, P. Vandenabeele, J. B. Prins, and J. R. Bradley.** 1999. Tumor necrosis factor induces distinct patterns of caspase activation in WEHI-164 cells associated with apoptosis or necrosis depending on cell cycle stage. Biochem. Biophys. Res. Commun. **261:**385–392.
11. **Flynn, J. L., J. Chan, K. J. Triebold, D. K. Dalton, T. A. Stewart, and B. R. Bloom.** 1993. An essential role for interferon γ in resistance to *Mycobacterium tuberculosis* infection. J. Exp. Med. **178:**2249–2254.
12. **Goossens, V., J. Grooten, K. de Vos, and W. Fiers.** 1995. Direct evidence for tumor necrosis factor-induced mitochondrial reactive oxygen intermediates and their involvement in cytotoxicity. Proc. Natl. Acad. Sci. USA **92:**8115–8119.
13. **Holler, N., R. Zaru, O. Micheau, M. Thome, A. Attinger, S. Valitutti, J.-L. Bodmer, P. Schneider, B. Seed, and J. Tschopp.** 2000. Fas triggers an alternative, caspase-8-independent cell death pathway using the kinase RIP as effector molecule. Nat. Immunol. **1:**489–495.
14. **Hsu, T., S. M. Hingley-Wilson, B. Chen, M. Chen, A. Z. Dai, P. M. Morin, C. B. Marks, J. Padiyar, C. Goulding, M. Gingery, D. Eisenberg, R. G. Russell, S. C. Derrick, F. M. Collins, S. L. Morris, C. H. King, and W. R. Jacobs, Jr.** 2003. The primary mechanism of attenuation of bacillus Calmette-Guérin is a loss of secreted lytic function required for invasion of lung interstitial tissue. Proc. Natl. Acad. Sci. USA **100:**12420–12425.
15. **Koul, A., T. Herget, B. Klebl, and A. Ullrich.** 2004. Interplay between mycobacteria and host signalling pathways. Nat. Rev. Microbiol. **2:**189–202.
16. **López, M., L. M. Sly, Y. Luu, D. Young, H. Cooper, and N. E. Reiner.** 2003. The 19-kDa *Mycobacterium tuberculosis* protein induces macrophage apoptosis through Toll-like receptor-2. J. Immunol. **170:**2409–2416.
17. **Matsumura, H., Y. Shimizu, Y. Ohsawa, A. Kawahara, Y. Uchiyama, and S. Nagata.** 2000. Necrotic death pathway in Fas receptor signaling. J. Cell Biol. **151:**1247–1255.
18. **Nicotera, P., and G. Melino.** 2004. Regulation of the apoptosis-necrosis switch. Oncogene **23:**2757–2765.
19. **Olleros, M. L., R. Guler, D. Vesin, R. Parapanov, G. Marchal, E. Martinez-Soria, N. Corazza, J.-C. Pache, C. Mueller, and I. Garcia.** 2005. Contribution of transmembrane tumor necrosis factor to host defense against *Mycobacterium bovis* Bacillus Calmette-Guerin and *Mycobacterium tuberculosis* infections. Am. J. Pathol. **166:**1109–1120.
20. **Park, J. S., M. H. Tamayo, M. Gonzalez-Juarrero, I. M. Orme, and D. J. Ordway.** 2006. Virulent clinical isolates of *Mycobacterium tuberculosis* grow rapidly and induce cellular necrosis but minimal apoptosis in murine macrophages. J. Leukoc. Biol. **79:**80–86.
21. **Riedl, S. J., and Y. Shi.** 2004. Molecular mechanisms of caspase regulation during apoptosis. Nat. Rev. Mol. Cell Biol. **5:**897–907.
22. **Riendeau, C. J., and H. Kornfeld.** 2003. THP-1 cell apoptosis in response to mycobacterial infection. Infect. Immun. **71:**254–259.
23. **Ryan, C. A., H. R. Stennicke, V. E. Nava, J. B. Burch, J. M. Hardwick, and G. S. Salvesen.** 2002. Inhibitor specificity of recombinant and endogenous caspase-9. Biochem. J. **366:**595–601.
24. **Saunders, B. M., S. Tran, S. Ruuls, J. D. Sedgwick, H. Briscoe, and W. J. Britton.** 2005. Transmembrane TNF is sufficient to initiate cell migration and granuloma formation and provide acute, but not long-term, control of *Mycobacterium tuberculosis* infection. J. Immunol. **174:**4852–4859.
25. **Schaible, U. E., F. Winau, P. A. Sieling, K. Fischer, H. L. Collins, K. Hagens, R. L. Modlin, V. Brinkmann, and S. H. E. Kaufmann.** 2003. Apoptosis facilitates antigen presentation to T lymphocytes through MHC-I and CD1 in tuberculosis. Nat. Med. **9:**1039–1046.
26. **Shiratsuchi, H., and J. J. Ellener.** 2001. Expression of IL-18 by *Mycobacterium avium*-infected human monocytes; association with *M. avium* virulence. Clin. Exp. Immunol. **123:**203–209.
27. **Slee, E. A., H. Zhu, S. C. Chow, M. MacFarlane, D. W. Nicholson, and G. M. Cohen.** 1996. Benzyloxycarbonyl-Val-Ala-Asp (OMe) fluoromethylketone (Z-VAD.FMK) inhibits apoptosis by blocking the processing of CPP32. Biochem. J. **315:**21–24.
28. **Sly, L. M., S. M. Hingley-Wilson, N. E. Reiner, and W. R. McMaster.** 2003. Survival of *Mycobacterium tuberculosis* in host macrophages involves resistance to apoptosis dependent upon induction of antiapoptotic Bcl-2 family member Mcl-1. J. Immunol. **170:**430–437.
29. **Stewart, G. R., B. D. Robertson, and D. B. Young.** 2003. Tuberculosis: a problem with persistence. Nat. Rev. Microbiol. **1:**97–105.
30. **Ulrichs, T., and S. H. E. Kaufmann.** 2006. New insights into the function of granulomas in human tuberculosis. J. Pathol. **208:**261–269.
31. **Vercammen, D., G. Brouckaert, G. Denecker, M. V. de Craen, W. Declercq, W. Fiers, and P. Vandenabeele.** 1998. Dual signaling of the Fas receptor: initiation of both apoptotic and necrotic cell death pathways. J. Exp. Med. **188:**919–930.
32. **Vercammen, D., R. Beyaert, G. Denecker, V. Goossens, G. V. Loo, W. Declercq, J. Grooten, W. Fiers, and P. Vandenabeele.** 1998. Inhibition of caspases increases the sensitivity of L929 cells to necrosis mediated by tumor necrosis factor. J. Exp. Med. **187:**1477–1485.

Editor: J. L. Flynn

RD1 region in mycobacterial genome is involved in the induction of necrosis in infected RAW264 cells via mitochondrial membrane damage and ATP depletion

Taijin Kaku, Ikuo Kawamura, Ryosuke Uchiyama, Takeshi Kurenuma & Masao Mitsuyama

Department of Microbiology, Kyoto University Graduate School of Medicine, Kyoto, Japan

Correspondence: Ikuo Kawamura, Department of Microbiology, Kyoto University Graduate School of Medicine, Yoshidakonoe-cho, Sakyo-ku, Kyoto 606-8501, Japan. Tel.: +81 75 753 4447; fax: +81 75 753 4446; e-mail: ikuo_kawamura@mb.med.kyoto-u.ac.jp

Received 8 March 2007; accepted 30 May 2007.

DOI:10.1111/j.1574-6968.2007.00838.x

Editor: Peter Andrew

Keywords
Mycobacterium tuberculosis; necrosis; RD1; mitochondria; ATP; RAW264 cells.

Abstract

It was shown that virulent *Mycobacterium tuberculosis* H37Rv induces necrosis of infected RAW264 cells at 24 h post infection while avirulent H37Ra and an attenuated H37Rv mutant that is deficient for RD1 region (H37RvΔ*RD1*) cause less necrosis of the infected cells. While H37Rv caused damage of the mitochondrial inner membrane and decreased the level of intracellular ATP, H37RvΔ*RD1* did not exhibit these harmful effects in infected cells. On the other hand, there was no difference in the level of intracellular reactive oxygen species after infection with H37Rv or H37RvΔ*RD1*, and the intracellular bacterial numbers of H37RvΔ*RD1* and H37Ra were comparable to that of H37Rv. These results suggested that some virulence factors of H37Rv may contribute to the necrosis of infected cells through induction of mitochondrial dysfunction and depletion of intracellular ATP. RD1 appeared to encode some components possibly playing a central role in the induction of host cell necrosis after *M. tuberculosis* infection.

Introduction

Macrophages are the primary target cells in the host infected with *Mycobacterium tuberculosis* (MTB). After infection into the cells of a macrophage lineage, MTB survives and multiplies inside cells by blocking the bactericidal mechanisms such as phagosomal acidification and phagosome–lysosome fusion. Host cells that cannot control the intracellular bacterial growth appear to be a comfortable niche for MTB. In this regard, apoptotic destruction of the infected macrophages has been proposed as a host defense mechanism to inhibit the spread of the disease process (Bocchino *et al.*, 2005). However, Keane *et al.* (2000) showed that virulent MTB is capable of growing inside macrophages by inhibition of cellular apoptosis.A recent report has shown that virulent MTB has a greater ability to cause necrosis of infected cells rather than does avirulent MTB (Chen *et al.*, 2006). In contrast to apoptosis, necrosis does not affect the intracellular growth of MTB and may allow acceleration of bacterial growth outside the cells (Sly *et al.*, 2003). These data indicate that the ability for apoptosis inhibition and necrosis induction is highly related to the virulence of MTB. This supports the concept that necrosis of cells by MTB infection is a major factor contributing to the pathogenesis of the disease process; however, the mechanism remains to be elucidated further.

The mitochondrion is an important organelle not only for ATP synthesis but also for the regulation of cell death including both apoptosis and necrosis (Armstrong, 2006). Marzo *et al.* (1998) reported that a damage to the mitochondrial outer membrane causes the release of cytochrome *c*, followed by apoptosis of cells through apoptosome formation and caspase activation. On the other hand, Nakagawa *et al.* (2005) showed that cells undergo necrosis when the inner membrane of the mitochondria is injured. In the case of MTB infection, virulent H37Rv caused necrosis of the infected cells through damage to the mitochondrial inner membrane whereas avirulent H37Ra did not exert such an activity (Chen *et al.*, 2006). The result strongly suggests that some gene products involved in the mitochondrial membrane damage may exist exclusively in H37Rv but not in H37Ra.

Recently, Behr *et al.* (1999) identified 16 deletions in the mycobacterial genome (designated region of difference, RD) that were present in MTB but absent in avirulent *Mycobacterium bovis* BCG. Mostowy *et al.* (2004) have shown that

the expression of genes at the RD1 locus is reduced in H37Ra compared with that in H37Rv. Hsu *et al.* (2003) have shown that the deletion of RD1 attenuates the virulence of MTB, while the severity of necrosis at the site of infection is alleviated when compared with the wild type. These results suggest strongly that RD1 may be essential in the induction of necrosis in the cells infected with MTB. In this study, based on the above findings, the necrosis-inducing ability of H37Rv and the mutant defective for RD1 was compared, it was found that the RD1 is involved in the induction of necrosis of the infected macrophages mainly by inducing damage of the mitochondrial inner membrane and causing ATP depletion.

Materials and methods

Bacterial strains

MTB H37Rv, mutant H37Rv strain deficient for the RD1 region (H37RvΔ*RD1*) and the complemented strain H37RvΔ*RD1* (pYUB412::*Rv3860–Rv3885c*) were kindly provided by Dr Tsungda Hsu Jr (Howard Hughes Medical Institute, NY) (Hsu *et al.*, 2003). H37Ra has been maintained in the authors' laboratory. These MTB strains were grown at 37 °C to the mid-log phase in Middlebrook 7H9 broth supplemented with 0.5% albumin, 0.2% dextrose, 3 μg mL^{-1} catalase and 0.2% glycerol. Bacteria were harvested, stirred vigorously with glass beads and centrifuged at 300 *g* for 3 min to remove the bacterial clumps, and then stored at −80 °C in aliquots. After thawing, the absence of bacterial clumps in the suspension was confirmed by Kinyoun staining. The viability of bacteria was determined in each experiment by counting the colonies after plating the diluted suspension on Middlebrook 7H10 agar plates containing 50 μg mL^{-1} oleic acid, 0.5% albumin, 0.2% dextrose, 4 μg mL^{-1} catalase and 0.85 mg mL^{-1} sodium chloride.

Enumeration of intracellular bacteria

RAW264 cells were obtained from the Riken Cell Bank (Ibaraki, Japan) and maintained in RPMI1640 medium supplemented with 10% fetal bovine serum. Cells were seeded in a 12-well culture plate at 1×10^5 cells well^{-1} and incubated for 12 h at 37 °C in the culture medium, washed and infected with 1×10^6 CFU of bacteria for 4 h. After washes, cells were cultured for 24 h in the presence of 5 μg mL^{-1} gentamicin and lysed in 0.05% Triton X-100 solution. The number of viable bacteria was enumerated by plating the cell lysate on Middlebrook 7H10 agar plates and colony counting after incubation for 21 days.

Detection of necrosis by measuring the release of lactate dehydrogenase (LDH) and propidium iodide (PI) staining

RAW264 cells (10^5) were infected with each strain of MTB (10^6 CFU) as described above and the culture supernatants were collected on the constant interval during 24 h. To monitor the degree of necrosis of the infected cells, the amount of LDH released from the infected cells was measured using an LDH Cytotoxicity Detection Kit (Takara Bio Inc., Shiga, Japan). The percentage of LDH released was calculated according to the following formula: % release = 100 × (experimental LDH release − spontaneous LDH release)/(maximal LDH release − spontaneous LDH release). A value of maximal LDH release was obtained from the supernatant of cells treated with 0.5% Triton X-100. Alternatively, RAW264 cells (10^5) were infected with MTB (10^6 CFU) for 24 h and stained with 0.2 mM PI for 5 min on ice. After washes with phosphate buffered saline (PBS), cells were fixed in 1% paraformaldehyde for 15 min and a fluorescence image was captured.

Measurement of DNA fragmentation

To detect apoptosis, RAW264 cells (10^5) were infected with each strain of MTB (10^6 CFU) and lysed 24 h after infection. Oligonucleosomes in the lysate were quantified using a Cell Death Detection ELISA^{PLUS} (Roche, Diagnostics, Penzberg, Germany) according to the manufacturer's protocol. The degree of DNA fragmentation was expressed as an arbitrary unit calculated by the following formula: Arbitrary unit = ($A_{405\,nm}$ of experimental group − $A_{405\,nm}$ of negative control (medium alone))/($A_{405\,nm}$ of untreated cells − $A_{405\,nm}$ of negative control).

Flow cytometric analysis

RAW264 cells (10^5) were infected with MTB (10^6 CFU) for varying periods and stained with 0.1 nM 3, 3′-dihexyloxycarbocyanine iodide $DiOC_6(3)$ (Molecular Probe, Eugene, OR) that emits the fluorescence after accumulation in the mitochondria (Korchak *et al.*, 1982). Cells were detached from the culture plates, washed and suspended in PBS containing 0.2% albumin. If the inner membrane of the mitochondria is damaged after MTB infection, the mitochondria are not able to retain $DiOC_6(3)$ any longer, resulting in the loss of fluorescence. Based on this, the integrity of mitochondrial inner membrane was assessed by measuring the fluorescence emission using a FACSCalibur (Becton Dickinson, Tokyo, Japan). To monitor the generation of intracellular reactive oxygen species (ROS), RAW264 cells were infected with MTB for 3 h and incubated with 5 μM dichlorodihydrofluorescein diacetate (DCFH-DA), which penetrates into the cytoplasm and emits fluorescence

when converted into oxidized form by intracellular ROS (Bass *et al.*, 1983). After washes, the fluorescence intensity of the cells was determined using the FACSCalibur.

Measurement of ATP level

RAW264 cells were infected with MTB as described above, washed once with PBS and lysed in 0.5% trichloroacetic acid. The amount of ATP in the cell lysate was determined using an ENLITEN® ATP Assay System Bioluminescence Detection Kit (Promega Corporation, Madison, WI). Chemiluminescence was measured by an ARVO SX 1420 multilabel counter (PerkinElmer, Boston, MA). The chemiluminescence detected by this procedure could be taken as ATP derived from RAW 264 cells, as no positive result was recorded in a sample of MTB without cells. The relative amount of ATP was expressed as an arbitrary unit calculated by the following formula: %ATP level = 100 × (relative light unit (RLU) of the experimental group − RLU of negative control (medium alone))/(RLU of untreated cells − RLU of negative control).

Statistical analysis

Student's *t*-test was used to determine the statistical significance of the values obtained, and a P value of < 0.05 was considered to be statistically significant.

Results and discussion

RD1 is involved in the necrosis of MTB-infected RAW264 cells

It has been reported that virulent MTB strains cause less apoptosis of infected human cells but induce necrosis compared with avirulent MTB strains (Sly *et al.*, 2003). To confirm the virulence-associated cytolytic effect of MTB on murine macrophages, first, necrosis-inducing ability toward RAW264 murine macrophage-like cells between virulent MTB H37Rv and attenuated H37Ra strains was compared. Cells were infected for 24 h and the amount of LDH released in the culture supernatant was determined as a representative marker of necrosis. Similar to human macrophages, a significant level of LDH release was observed in the culture supernatant of H37Rv-infected cells but not in that of noninfected cells (Fig. 1a). The level of LDH release in the cells infected with H37Ra was substantially lower than that with H37Rv. It was confirmed that virulent H37Rv possesses a higher activity to cause necrosis in RAW264 cells than that of avirulent H37Ra.

Recent studies have shown that mutant H37Rv deficient for RD1 exhibits an attenuated virulence compared with H37Rv, and hardly induces necrosis of the lung in infected mice (Hsu *et al.*, 2003; Junqueira-Kipnis *et al.*, 2006).

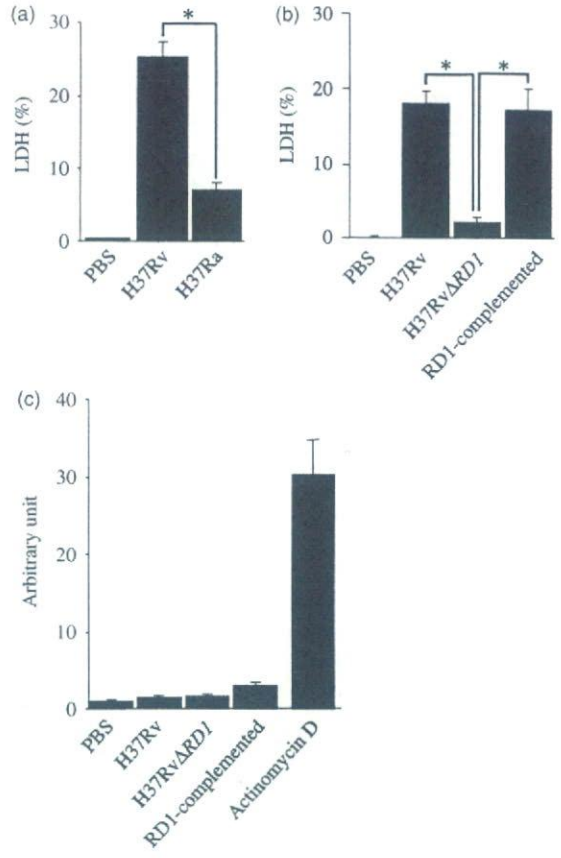

Fig. 1. LDH release and oligonucleosome formed in the cells infected with H37Rv, H37Rv*ΔRD1* and RD1-complemented strains. RAW264 cells were infected with the MTB strains at MOI of 10 for 4 h and the amount of LDH was measured 24 h later. (a) LDH activity in the culture supernatant of cells infected with H37Rv and H37Ra. (b) LDH activity in the culture supernatant of cells infected with H37Rv, H37Rv*ΔRD1* and RD1-complemented strains. (c) Cells were infected with H37Rv, H37Rv*ΔRD1* and RD1-complemented strains, or incubated with 1 μg mL^{-1} actinomycin D for 24 h. The cell lysate was prepared and the amount of oligonucleosomes was determined. Data represent the mean ± SD of triplicate assays and are representative of three independent experiments.

Although the RD1 locus is also present in H37Ra, it has been shown that the expression of genes at RD1 is reduced when compared with that of H37Rv (Mostowy *et al.*, 2004). These findings prompted investigation of whether the RD1 of MTB is involved in the induction of necrosis in RAW264 cells after infection. To test this possibility, RAW264 cells were infected with H37Rv, H37Rv*ΔRD1* and H37Rv*ΔRD1* complemented with RD1 for 24 h, and LDH released in the supernatant was measured. As shown in Fig. 1b, a high level of LDH release was induced by H37Rv, but not by H37Rv*ΔRD1*. As expected, the impaired activity of the deficient mutant to induce LDH release was restored by complementation with RD1.

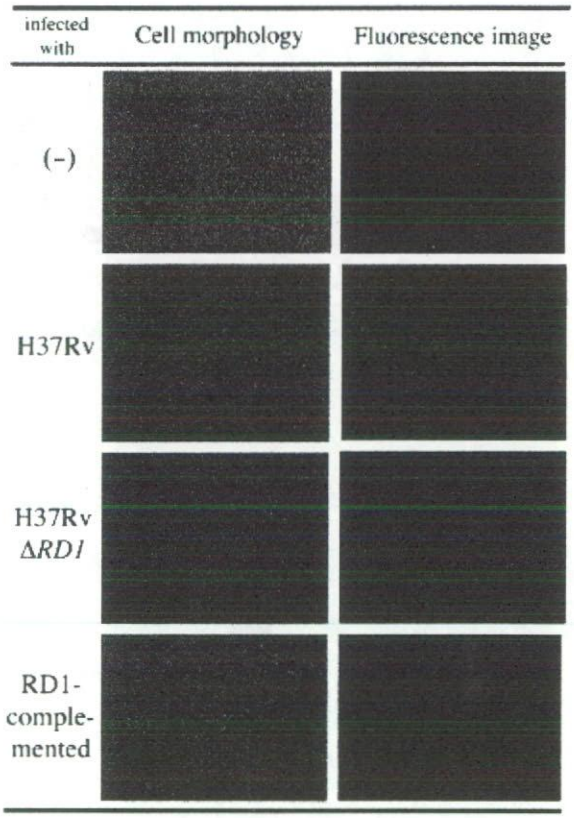

Fig. 2. PI staining of RAW264 cells infected with H37Rv, H37RvΔ*RD1* and RD1-complemented strains. RAW264 cells were infected with the MTB strains for 24 h and stained with PI. The cells were observed in bright field (left) and the fluorescence image was detected under UV excitation light (right). Data are representative of three independent experiments.

To rule out the possible contribution of apoptotic cell death to the LDH release, the amount of oligonucleosomes in the infected cells was quantified 24 h after infection with each MTB strain. Compared with the level of apoptosis induced by treatment with actinomycin D as a positive control, only a marginal increase was seen after infection, but there was no difference among three groups (Fig. 1c). Next, cells were stained with PI 24 h after infection to analyze the population of PI-stained cells using a fluorescence microscope. Under this experimental condition, there was no significant difference in the proportion of cells infected with bacteria among these three groups (data not shown). Most of the cells infected with H37Rv became PI-positive (Fig. 2). No PI-positive cell could be observed after infection with H37RvΔ*RD1*, and an image nearly similar to the infection with H37Rv was obtained in cells infected with the RD1-complemented strain of H37RvΔ*RD1*. This finding clearly indicated that the cell death induced by H37Rv was not due to apoptosis. The RD1 region of MTB appeared to be critically important for the induction of a necrosis type of host cell death upon infection.

RD1-dependent damage of the inner membrane of mitochondria in infected cells

It has been shown that H37Rv but not H37Ra injures the inner membrane of the mitochondria, resulting in the necrosis of infected macrophages (Chen *et al.*, 2006). In the present experiment, it was next examined whether H37Rv causes any damage to the mitochondria of RAW264 cells in a manner that depends on the presence of RD1. RAW264 cells were infected with H37Rv, H37RvΔ*RD1* and its RD1-complemented strain for 2–24 h, and stained with $DiOC_6(3)$ to assess the integrity of mitochondrial inner membrane. Noninfected cells showed a single-peaked profile due to the accumulation of fluorescent dye inside the inner membrane of the mitochondria. The shift of the profile to a lower intensity was regarded as the result of inner membrane damage, followed by the loss of dye accumulation. Compared with the intensity of uninfected cells, the peak of fluorescence was diverse. A similar change in the FACS profile was detected as early as 2 h after infection with H37Rv or H37RvΔ*RD1* complemented with RD1 (Fig. 3). At this time point, the cell population expressing lower fluorescence (M2) was 30% or 31% of the total cells infected with H37Rv or H37RvΔ*RD1*complemented with RD1, respectively. The population of the cells that lost an intact level of fluorescence was gradually increased during the 24 h (38% in H37Rv-infected cells and 55% in those infected with the RD1-complemented strain). Such a significant change was not observed in the cells infected with H37RvΔ*RD1*, and almost the same intact profile as in noninfected cells was maintained for 24 h after infection. To rule out the possibility that the significant differences observed between H37Rv and H37RvΔ*RD1* were simply due to the difference in the number of bacteria that infected and replicated intracellularly for 24 h, the number of bacteria during the culture period was compared. At the beginning of culture, there was no significant difference in the number of infected bacteria among all the groups (Table 1). The bacteria grew gradually and showed a similar growth rate during the 24-h culture. The values in fold-increase calculated at 24 h of culture for each group were 2.9, 2.5 and 2.1 for H37Rv, H37RvΔ*RD1* and H37RvΔ*RD1* complemented with RD1, respectively. Although there was some difference in the values expressed in the fold-increase, it was clear that the small difference in bacterial growth could never account for the significant level of difference in the cytotoxic effect observed in this study.

It has been shown that the RD1 locus contains genes coding for the components of the secretory machinery and two secretory molecules, designated as 'early secreted

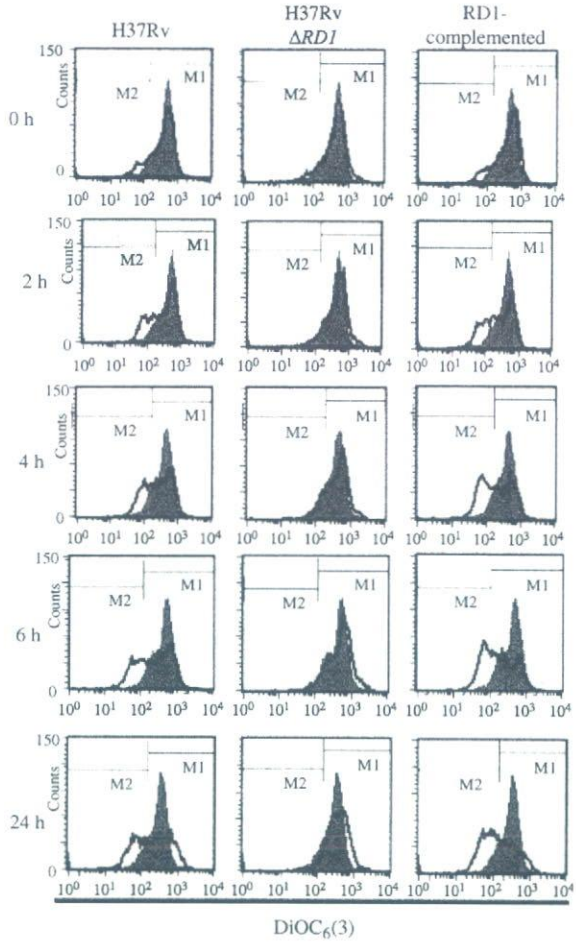

Fig. 3. Measurement of mitochondrial injury in RAW264 cells after infection with H37Rv, H37Rv*ΔRD1* and RD1-complemented strains. RAW264 cells were infected with the MTB strains at MOI of 10 for 4 h. Thereafter, cells were collected at the indicated times after infection and stained with $DiOC_6(3)$. The fluorescence intensity was measured by FACS. The shaded peak represents the fluorescence intensity of cells without infection. The bold line indicates the fluorescence profile of the MTB-infected cells. Data are representative of three independent experiments.

Table 1. Comparison of intracellular growth of H37Rv, H37Rv*ΔRD1* and RD1-complemented strain in RAW264 cells

	MTB ($\times 10^5$ CFU) well^{-1}*	
Bacteria	0 day	1 day
H37Rv	3.3 ± 0.5	9.6 ± 1.2
H37Rv*ΔRD1*	4.0 ± 0.1	9.8 ± 0.7
RD1-complemented	3.4 ± 1.4	7.3 ± 1.7

*RAW264 cells were infected with the MTB strains at MOI of 10 for 4 h. After washes, cells were lysed immediately (0 day) and 1 day after cultivation in 0.05% Triton X-100, and the CFU number was determined. Data represent the mean ± SD of triplicate assays and are representative of three independent experiments.

antigen of tuberculosis 6' (ESAT-6) and 'culture filtrate protein 10' (CFP-10) (Berthet *et al.*, 1998). It has been shown that ESAT-6 alone or in combination with CFP-10 may cause disintegration of the plasma membrane (Hsu *et al.*, 2003) and that some mycobacterial proteins are capable of penetrating through the phagosomal membrane in infected macrophages (Teitelbaum *et al.*, 1999). Thus, it is probable that ESAT-6 and CFP-10 may be secreted in the cytoplasm and contribute to the induction of mitochondrial membrane damage, whereas the expression of ESAT-6 and CFP-10 is reported to be downregulated in phagosome (Schnappinger *et al.*, 2003). Alternatively, it has been shown that the complex of these proteins binds specifically to the cell membrane of the macrophages (Renshaw *et al.*, 2005). The interaction of host cells with mycobacterial products may cause mitochondrial membrane damage; however, the more exact mechanism remains to be elucidated.

H37Rv infection causes depletion of ATP but does not affect generation of ROS in the cytoplasm

It has been shown that destruction of the mitochondrial inner membrane affects electron transport and oxidative phosphorylation, resulting in the depletion of ATP and an increase of ROS generation in the cytoplasm (Skulachev, 2006). A recent study also demonstrated that reduction of intracellular ATP level and an increase in intracellular ROS are the causes of necrotic cell death in infection with *Shigella flexneri* (Koterski *et al.*, 2005). Consequently, it was investigated whether intracellular ROS is generated by H37Rv infection and contributes to the induction of necrosis. RAW264 cells were infected with H37Rv, H37Rv*ΔRD1* and RD1-complemented strains, and the generation of intracellular ROS was evaluated by measuring the fluorescence intensity of DCFH-DA, an indicator for intracellular ROS. The three MTB strains similarly enhanced the fluorescence intensity 3 h after infection (Fig. 4a). Butylated hydroxyanisole (BHA), a scavenger of ROS, diminished these fluorescence emissions, indicating that a similar level of intracellular ROS was generated after infection with these MTB strains (Fig. 4b). However, H37Rv and H37Rv*ΔRD1* complemented with RD1 caused a decrease in the fluorescence of $DiOC_6(3)$ but H37Rv*ΔRD1* did not (Fig. 4c). Moreover, the shift of fluorescence peak was not restored by BHA while intracellular ROS was mostly abolished (Fig. 4d). It has been shown that overproduction of ROS by the mitochondria causes necrosis (Goossens *et al.*, 1995). However, Lee *et al.* (2006) reported that macrophages eventually undergo necrosis in response to a high intracellular burden of MTB without participation of intracellular ROS. Although ROS was detected after infection with H37Rv strains in this study, ROS was unlikely to be involved in the

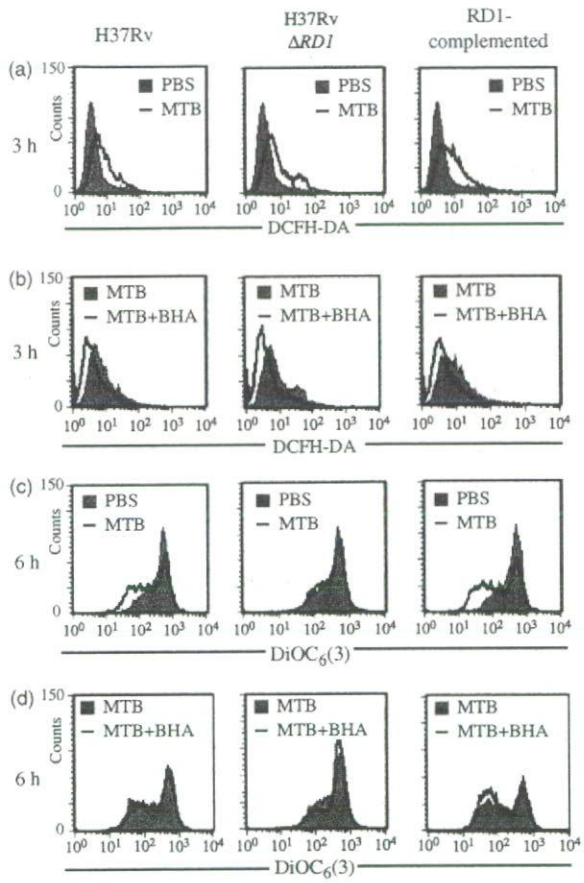

Fig. 4. Generation of ROS in RAW264 cells infected with H37Rv, H37RvΔ*RD1* and RD1-complemented strains. RAW264 cells were infected with the MTB strains at an MOI of 10 for 3 h in the absence (a) or presence (b) of BHA. Cells were incubated with DCFH-DA and the fluorescence intensity was measured. RAW cells were infected with the MTB strains for 6 h in the absence (c) or presence (d) of BHA. Cells were incubated with $DiOC_6(3)$ and the fluorescence intensity was measured. Data are representative of three independent experiments.

mitochondrial injury of the infected cells. Therefore, it seems that MTB does not induce ROS generation by mitochondria.

Next, the amount of intracellular ATP was measured to examine whether the change in the intracellular ATP level plays a role in the necrosis of H37Rv-infected cells. Figure 5 clearly shows that the level of ATP was reduced by $< 50\%$ when cells were infected with H37Rv and an RD1-complemented strain for 6 h, but such a change was not observed when cells were infected with H37RvΔ*RD1*. Kinetic study revealed that the decline in the ATP level was detected as early as 2 h after the infection and was maintained at least for 6 h (data not shown). The reduction of ATP did not appear to be due to the difference in the condition of bacteria, because RAW264 cells were infected with single

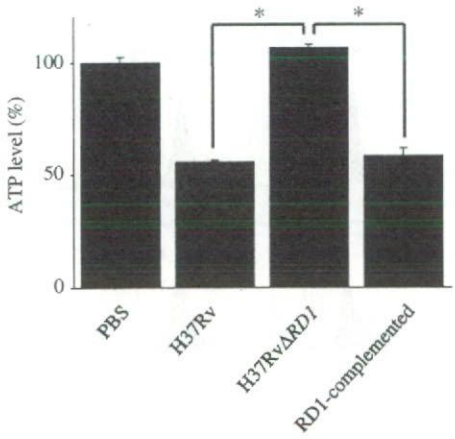

Fig. 5. Determination of intracellular ATP level in RAW264 cells infected with H37Rv, H37RvΔ*RD1* and RD1-complemented strains. RAW264 cells were infected with the MTB strains at an MOI of 10 for 6 h and the level of intracellular ATP was determined. Data represent the mean ± SD of triplicate assays and are representative of three independent experiments.

cells of MTB strains that were highly viable. Koterski *et al.* (2005) showed that virulent *Shigella* caused a rapid reduction of the ATP level to about 50% and triggered necrosis of the infected macrophages. Therefore, it is likely that the change of ATP level may account for the necrosis of MTB-infected cells.

Taken together, the results presented in this study suggested strongly that H37Rv, a virulent strain of MTB, is capable of affecting the inner membrane of mitochondria resulting in the induction of necrotic-type death of host cells in a manner dependent on the RD1 locus. The RD1-dependent cellular necrosis appeared due to the depletion of intracellular ATP. The present study may have provided important findings that extend the understanding of the molecular mechanism involved in the pathology of infection with MTB.

Acknowledgements

This work was supported by a Grant-in-Aid for Scientific Research on Priority Areas from the Ministry of Education, Science, Culture and Sports of Japan, Grant-in-Aid for Scientific Research (B) and (C) from The Japan Society for the Promotion of Science and in part by a Grant-in Aid for Scientific Research from the Ministry of Health, Labor and Welfare, Japan.

References

Armstrong JS (2006) Mitochondrial membrane permeabilization: the sine qua non for cell death. *BioEssays* **28**: 253–260.

Bass DA, Parce JW, Dechatelet LR, Szejda P, Seeds MC & Thomas M (1983) Flow cytometric studies of oxidative product formation by neutrophils: a graded response to membrane stimulation. *J Immunol* **130**: 1910–1917.

Behr MA, Wilson MA, Gill WP, Salamon H, Schoolnik GK, Rane S & Small PM (1999) Comparative genomics of BCG vaccine by whole-genome DNA microarray. *Science* **284**: 1520–1523.

Berthet FX, Rasmussen PB, Rosenkrands I, Andersen P & Gicquel B (1998) A *Mycobacterium tuberculosis* operon encoding ESAT-6 and a novel low-molecular-mass culture filtrate protein (CFP-10). *Microbiology* **144**: 3195–3203.

Bocchino M, Galati D, Sanduzzi A, Colizzi V, Brunetti E & Mancino G (2005) Role of mycobacteria-induced monocyte/macrophage apoptosis in the pathogenesis of human tuberculosis. *Int J Tuberc Lung Dis* **9**: 375–383.

Chen M, Gan H & Remold HG (2006) A mechanism of virulence: *Mycobacterium tuberculosis* strain H37Rv, but not attenuated H37Ra, causes significant mitochondrial inner membrane disruption in macrophage leading to necrosis. *J Immunol* **176**: 3707–3716.

Goossens V, Grooten J, De Vos K & Fiers W (1995) Direct evidence for tumor necrosis factor-induced mitochondrial reactive oxygen intermediates and their involvement in cytotoxicity. *Proc Natl Acad Sci USA* **92**: 8115–8119.

Hsu T, Hingley-Wilson SM, Chen B *et al.* (2003) The primary mechanism of attenuation of Bacillus Calmette–Guérin is a loss of secreted lytic function required for invasion of lung interstitial tissue. *Proc Natl Acad Sci USA* **100**: 12420–12425.

Junqueira-Kipnis AP, Basaraba RJ, Gruppo V *et al.* (2006) Mycobacteria lacking the RD1 region do not induce necrosis in the lungs of mice lacking interferon-γ. *Immunology* **119**: 224–231.

Keane J, Remold HG & Kornfeld H (2000) Virulent *Mycobacterium tuberculosis* strains evade apoptosis of infected alveolar macrophages. *J Immunol* **164**: 2016–2020.

Korchak HM, Rich AM, Wilkenfeld C, Rutherford LE & Weissmann G (1982) A carbocyanine dye, $DiOC_6(3)$, acts as a mitochondrial probe in human neutrophils. *Biochem Biophys Res Commun* **108**: 1495–1501.

Koterski JF, Nahvi M, Venkatesan MM & Haimovich B (2005) Virulent *Shigella flexineri* causes damage to mitochondria and triggers necrosis in infected human monocyte-derived macrophages. *Infect Immun* **73**: 504–513.

Lee J, Remold HG, Ieong MH & Kornfeld H (2006) Macrophage apoptosis in response to high intracellular burden of *Mycobacterium tuberculosis* is mediated by a novel caspase-independent pathway. *J Immunol* **176**: 4267–4274.

Marzo I, Brenner C, Zamzami N, Susin SA, Buetner G, Brdiczka D, Remy R, Xie ZH, Reed JC & Kroemer G (1998) The permeability pore complex: a target for apoptosis regulation by caspases and Bcl-2-related proteins. *J Exp Med* **187**: 1261–1271.

Mostowy S, Cleto C, Sherman DR & Behr MA (2004) The *Mycobacterium tuberculosis* complex transcriptome of attenuation. *Tuberculosis* **84**: 197–204.

Nakagawa T, Shimizu S, Watanabe T, Yamaguchi O, Otsu K, Yamagata H, Inohara H, Kubo T & Tsujimoto Y (2005) Cyclophilin D-dependent mitochondrial permeability transition regulates some necrotic but not apoptotic cell death. *Nature* **434**: 652–658.

Renshaw PS, Lightbody KL, Veverka V *et al.* (2005) Structure and function of the complex formed by the tuberculosis virulence factors CFP-10 and ESAT-6. *EMBO J* **24**: 2491–2498.

Schnappinger D, Ehrt S, Voskuil MI *et al.* (2003) Transcriptional adaptation of *Mycobacterium tuberculosis* within macrophages: insights into the phagosomal environment. *J Exp Med* **198**: 693–704.

Skulachev VP (2006) Bioenergetic aspects of apoptosis, necrosis and mitoptosis. *Apoptosis* **11**: 473–485.

Sly LM, Hingley-Wilson SM, Reiner NE & McMaster WR (2003) Survival of *Mycobacterium tuberculosis* in host macrophages involves resistance to apoptosis dependent upon induction of antiapoptotic Bcl-2 family member Mcl-1. *J Immunol* **170**: 430–437.

Teitelbaum R, Cammer M, Maitland ML, Freitag NE, Condeelis J & Bloom BR (1999) Mycobacterial infection of macrophages results in membrane-permeable phagosomes. *Proc Natl Acad Sci USA* **96**: 15190–15195.

EXPERIMENTAL MEDICINE
実験医学 増刊

別　刷

羊土社

〒101-0052
東京都千代田区神田小川町2-5-1
TEL 03(5282)1211　FAX 03(5282)1212
E-mail：eigyo@yodosha.co.jp

7. 抗結核防御免疫と結核菌による免疫制御

河村 伊久雄，光山正雄

結核菌感染宿主では，抗原特異的Th1型T細胞の分化が誘導され，結核菌に対する強い感染防御免疫が出現する．しかし，結核菌は防御免疫が成立しても容易に感染宿主体内から排除されず，長期間生存し続けることができる．結核を撲滅するためにはこの機序を明らかにする必要があるが，いまだ解明には至っていない．本稿では，宿主感染防御免疫の全体像を示すとともに，菌がどのようにして宿主防御免疫に抵抗し，体内で生在し続けるのかについてこれまでに明らかにされたことを示す．

はじめに

結核は世界的に見て今なお単一の病原体による最大の感染症である．WHOはこれまでに世界の約3割が結核の感染を受け，毎年約880万人の結核患者が発生し，約158万人が結核で死亡していると推定している（www.who.int/tb/publications/global_report）．結核患者の発生はアフリカおよびアジアなどの発展途上国に多くみられるが，多剤耐性結核菌の出現頻度の増加や，結核蔓延国からの人的流入などにより，先進国においても今後結核の増加が懸念される現状にある．我が国においては，これまで減少を続けてきた結核の新規罹患率，有病率が増加に転じ，1999年には厚生省（現，厚生労働省）から結核緊急事態宣言が出されるに至った．現在我が国の結核罹患率は米国の約5倍，欧米主要国の数倍を下らないことから，結核は現在もなお脅威であることを認識する必要がある．

結核菌（*Mycobacterium tuberculosis*）は生体内で

[キーワード&略語]
結核菌，マクロファージ，樹状細胞（DC），T細胞，サイトカイン

ICL：isocitrate lyase（イソクエン酸リアーゼ）
IFN-γ：interferon-γ（ガンマ－インターフェロン）
LAM：lipoarabinomannan（リポアラビノマンナン）
MCP-1：monocyte chemoattractant protein-1（単球走化性因子）
MIP1-α：macrophage migration inhibitory protein 1-α（マクロファージ遊走阻止因子）
PI3K：phosphatidylinositol 3-kinase（フォスファチジルイノシトール3キナーゼ）
PIM：phosphatidylinositolmannoside（フォスファチジルイノシトールマンノシド）
RANTES：regulated on activation normally T-cell expressed and secreted
TLR：Toll-like receptor（Toll様受容体）
TNF-α：tumor necrosis factor-α（腫瘍壊死因子）

Anti-mycobacterial immunity and the regulatory mechanism of immune response by *Mycobacterium tuberculosis*

Ikuo Kawamura/Masao Mitsuyama：Department of Microbiology, Graduate School of Medicine, Kyoto University（京都大学大学院医学研究科微生物感染症学）

は細胞内寄生性を示し，マクロファージに貪食されてもその細胞内殺菌機構に抵抗して，細胞内で長期間生存することができる．多くの場合，結核菌はそのまま増殖せずにヒトと共存するが，5～10％の感染宿主で結核が再燃し，成人にみられる慢性結核を発症する．ヒトと結核菌は長い共存の歴史があり，旧来より菌がどのようにして宿主防御免疫に抵抗して生在し続けるのかという問題について精力的な研究がなされてきたが，その疑問を解決するには至らなかった．しかし，1998年に結核菌の全塩基配列が決定されたことが転機となり[1]，現在では菌の病原性に重要と考えられるいくつかの因子が同定されている．また最近，結核に対する感染防御には$CD4^+$T細胞や$CD8^+$T細胞以外に，Th17細胞や制御性T細胞が関与することが示されており，抗結核防御免疫がさまざまなT細胞によって形成された複雑なネットワークのうえに成り立っていることが示唆されている．

1 結核菌の感染動態

1）結核菌の細胞内寄生メカニズム

結核菌は宿主体内に侵入後，肺胞マクロファージ，樹状細胞（dendritic cell：DC）あるいは単球に積極的に侵入する．この細胞内侵入にはマクロファージ表面の補体受容体，マンノース受容体，Fc受容体，フィブロネクチンあるいはスカベンジャー受容体などが関与する[2]．これら細胞表面受容体を介した結核菌の細胞内侵入は，マクロファージの殺菌機構や，感染防御に関与するTh1型サイトカイン産生を亢進しないことが示されており，これら細胞表面受容体を介した食細胞と菌とのinteractionは，結核菌が宿主初期防御反応を刺激せずに細胞内寄生を成立させるための重要なメカニズムであると考えられる[3)4)]．また，結核菌は菌体表面のmycobacterial mammalian cell entry protein 1Aやmycobacterial DNA-binding protein 1を介して非貪食細胞である肺胞上皮細胞に侵入することができる[5)6)]．感染した病原体を排除する能力が弱い上皮細胞への侵入は，結核菌の宿主体内での長期生存をより容易にするものと考えられる．

マクロファージに侵入した菌はファゴソーム内で生存増殖する．通常，ファゴソームの成熟が進むとファゴソームはリソソームと融合してファゴリソソームが形成される．このファゴリソソーム内の環境は結核菌にとっても殺菌的である．しかし，結核菌はファゴリソソーム形成を阻害し，ファゴソーム内の環境を自身の生存に適したものに変えてしまう．この抑制機序には，結核菌由来のLAM（lipoarabinomannan）とlipid phosphataseであるSapMが重要な役割を果たしている[7]．ファゴソームとリソソームの融合にはPI3K（phosphatidylinositol 3-kinase）により合成されるファゴソーム膜上のPI3P（phosphatidylinositol 3-phosphate）が重要であるが，LAMは細胞内$Ca2^+$濃度の上昇を抑えることでPI3Kのファゴソームへの動員を抑制し，ファゴソーム膜上のPI3Pの合成を阻害する．また，SapMはPI3Pの脱リン酸化を引き起こすことで，ファゴリソソーム形成を抑制することが示されている．これらに加えて，Jayachandranらは，マクロファージに存在するcoronin 1が結核菌を含むファゴソームに集積し，$Ca2^+$依存性脱リン酸酵素カルシニューリンが活性化することでファゴリソソーム融合が阻害されることを明らかにした[8]．（図1）さらに最近，結核菌を感染させたマクロファージにオートファジー※1を誘導すると，細胞内菌数が減少することが示された．オートファジーは，細胞の恒常性維持に必要と考えられてきた機構であるが，この結果は，オートファジー経路が結核菌の細胞内殺菌にも関与することを示すものである[9)10)]．しかし，結核菌感染マクロファージにオートファジーを誘導するためには，IFN-γ（interferon-γ）でマクロファージを活性化する必要があることから，結核菌はオートファジーの誘導に必要なPI3K活性を抑制することで，ファゴリソソーム融合だけでなく，オートファジー経路も抑制していることが示唆される．

このようなマクロファージの細胞内殺菌に対する抵抗性に加えて，結核菌強毒株はマクロファージのアポトーシスを抑制するメカニズムを有することが示されている[11)12)]．感染マクロファージがアポトーシスに陥ると菌の細胞内増殖が抑制され，カスパーゼ阻害剤を用いてアポトーシス誘導を阻害すると菌の細胞内増殖が回復することから，アポトーシスは結核菌に対する

※1 オートファジー

細胞内のタンパク質を分解するための機構．細胞内での異常なタンパク質の蓄積を防いだり，過剰にタンパク質を合成したときや栄養環境が悪化したときにタンパク質のリサイクルを行い，生体の恒常性維持に関与している．

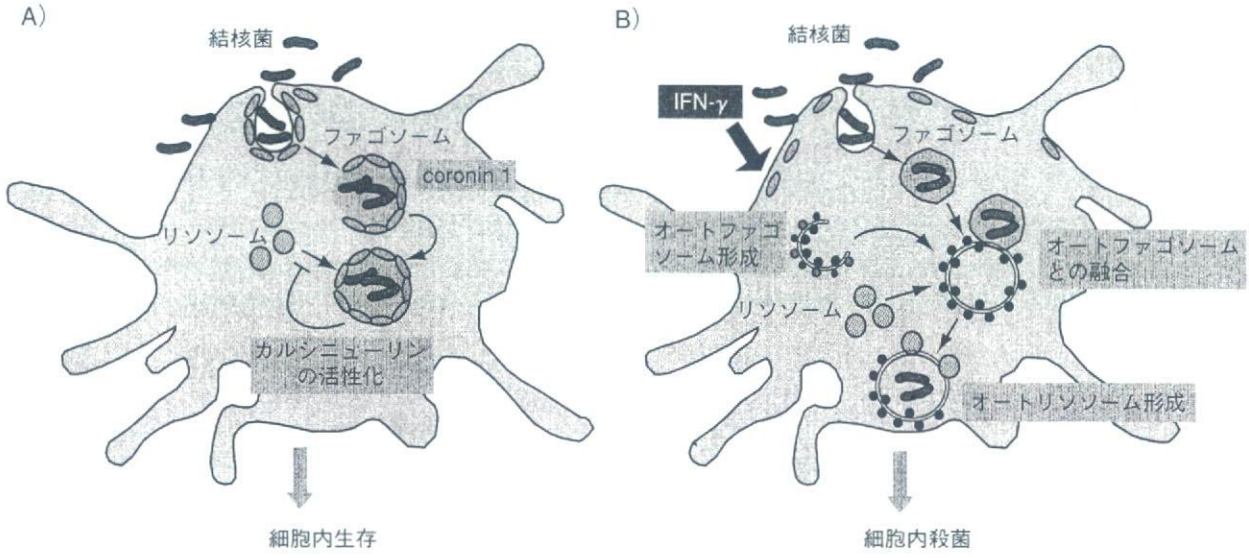

図1　結核菌の細胞内殺菌抵抗性とオートファジーによる殺菌機構
A）結核菌を含むファゴソームにはcoronin 1分子が集積しカルシニューリンが活性化されると，ファゴリソソーム形成が阻害され，菌は細胞内で生存することができる．B）IFN-γでマクロファージを刺激するとオートファゴソーム形成が誘導される．オートファゴソームは結核菌を含むファゴソームと融合し，最終的にオートリソソームが形成され，細胞内の菌は殺菌処理される

宿主側の初期防御反応と捉えることができる．したがって，結核菌の有するアポトーシス抑制活性は，増殖の場を確保するという意味で重要な機序であり，細胞内寄生を可能にするために必須であると考えられる．

2）感染成立後の結核菌の抵抗性

さらに感染が進むと，感染病巣部には肉芽腫が形成される．これは感染の拡大を防ぐための一種の封入組織であり，菌を貪食したマクロファージを中心にその周りをランゲルハンス巨細胞，リンパ球やマクロファージが取り囲んだ構造をしている．肉芽腫内部，あるいは宿主組織内は酸素分圧が低く，偏性好気生菌である結核菌には非常に苛酷な環境と考えられる．しかし，結核菌はその代謝系を環境に適応したものに切り替えて細胞内での生存を可能にしていることが示されており，その結果パーシスターとして休眠状態（dormancy）へと移行するものと考えられる[13]．McKlenneyらは，結核菌が肺で持続感染を成立させるためにはイソクエン酸リアーゼ（isocitrate lyase：ICL）が重要な役割を果たすことを示した[14]．ICLは，脂質を材料とした糖の生合成経路，グリオキシル酸サイクルの酵素の1つである．肉芽腫内に存在する結核菌のICL活性が菌の生存に重要であるということは，菌が酸素分圧の低い環境では脂質を炭素源として利用することを示すものである．その他にも低酸素条件で誘導される遺伝子として熱ショックタンパク質の一種であるα-クリスタリンやnitrate reductase，またはEisやKatGなどが細胞内増殖や持続感染に関与する因子として報告されており，菌がパーシスターとして存在するためには非常に複雑なメカニズムが働いていると思われる．（表1）

宿主防御システムが一旦低下しはじめると，休眠状態に移行した菌が再び増殖を始め，結核が再燃する．この場合，菌の増殖が認められた組織には，ネクローシスに陥った細胞が多数認められる．これまでの解析から，菌の病原性とネクローシス誘導能には関連があり，細胞内で増殖した菌が感染細胞を破壊し，細胞外に出て感染を拡大するためには，感染細胞のネクローシス誘導が重要なステップであると考えられている．さらに，分子レベルの解析の結果，結核菌による感染マクロファージのネクローシス誘導には結核菌ゲノム上のRD1[※2]領域が重要な役割を果たしており，この領域に存在する遺伝子産物が，ミトコンドリア膜障害を引き起こし，細胞内ATP濃度が減少するため，細胞がネクローシスに陥ることが示されている[15]．また，

表1　結核菌の持続感染および細胞内寄生に関連する遺伝子

遺伝子番号	遺伝子	機能	文献
Rv0353	*hspR*	転写阻害	Nat. Med., 7：732-727, 2001
Rv0467	*icl*	イソクエン酸リアーゼ	Nature, 406：735-738, 2000
Rv0470c	*pcaA*	シクロプロパンシンターゼ	Mol. Cell, 5：717-727, 2000
Rv0981	*mprA*	2成分制御系	Proc. Natl. Acad. Sci. USA, 98：12706-12711, 2001
Rv1027/8c	*kdpDE*	2成分制御系	Infect. Immun., 71：1134-1140, 2003
Rv1032c	*trcS*	2成分制御系	Infect. Immun., 71：1134-1140, 2003
Rv1161-4	*narGHJI*	nitrate reductase	Infect. Immun., 70：286-291, 2002
Rv1651c/3812	*mag24-1*	PE-PGRS	Science, 288：1436-1439, 2000
Rv1736v	*narX*	fused nitrate reductase	Infect. Immun., 70：6330-6338, 2002
Rv1737c	*narK2*	亜硝酸塩／硝酸塩トランスポーター	FEMS Microbiol. Lett., 188：141-146, 2000
Rv1908c	*katG*	カタラーゼ／ペルオキシダーゼ	J. Infect.Dis., 177：1030-1035, 1998
Rv2031c	*hspX*	α-クリスタリン	J. Bacteriol., 178：4484-4492, 1996
Rv2583c	*relA*	GTP ピロホスホキナーゼ	J. Bacteriol., 182：4889-4898, 2000
Rv3132c	*devR*	2成分制御系	Infect. Immun., 71：1134-1140, 2003
Rv3286c	*sigF*	RNA ポリメラーゼσ因子	Infect. Immun., 68：5575-5580, 2000
Rv3764/5c	*tcrXY*	2成分制御系	Infect. Immun., 71：1134-1140, 2003

結核菌が細胞内増殖する感染初期には，菌はカスパーゼ9の活性化を誘導してネクローシスを抑制することが明らかにされている[16]．このような結核菌による感染マクロファージのプログラムされた細胞死の制御が，生体内での生存増殖に寄与するところは大きいと考えられる．

2 結核菌に対する感染防御

1）初期感染防御反応

マクロファージやDCの感染局所への動員，あるいは結核菌貪食後のマクロファージの活性化は結核菌に対する初期防御反応だけでなく，特異的免疫応答の誘導においても重要である．マクロファージやDCは細胞表面のTLR（Toll-like receptor）を介して結核菌を認識する．TLR2は結核菌の主要な細胞壁リポ多糖体成分であるLAM，フォスファチジルイノシトールマンノシド（phosphatidylinositolmannoside：PIM）あるいは19 kDaリポタンパク質を認識することが示されている．また，易熱性結核菌体抗原はTLR4により識別される．その結果，マクロファージやDCが活性化され，炎症性サイトカインが産生される．また，19 kDaリポタンパク質を介したTLR2の刺激はマクロファージのアポトーシスを誘導することや，TLR4リガンドの刺激が，オートファジーを誘導することが最近明らかとなり，これら結核菌成分とTLRリガンドのinteractionが，細胞死を介した初期防御反応の誘導にも関与することが示されている[17) 18)]．一方，病原性の強い結核菌やBCGのLAMはその先端にマンノース残基が付加しており（Man-LAM），非定型抗酸菌のLAMとは構造的に異なる．このMan-LAMはTLR2分子を介したマクロファージの活性化を誘導せず，これが結核菌の病原性において重要なメカニズムの1つと考えられる[19]．

結核菌を貪食し，活性化したマクロファージはRANTES（regulated on activation normally T-cell expressed and secreted），MIP1-α（macrophage

※2　RD1

結核菌と弱毒ワクチン株である*M. bovis* BCG株のゲノムを比較し，BCGで欠落している結核菌の遺伝子領域をRD（region of difference）領域と呼ぶ．現在，16領域が確認されており，そのうちRD1が菌の病原性に深く関係していることが明らかにされている．

migration inhibitory protein 1-α), MIP2, MCP-1 (monocyte chemoattractant protein-1), MCP-3, MCP-5, IP-10などのケモカインを産生し，感染局所への炎症性細胞を動因する．（図2）また，感染マクロファージが産生するサイトカインのうち，TNF-α (tumor necrosis factor), IL-1 (interleukin-1), IL-12やIL-18はマクロファージを活性化し，肉芽腫形成や感染初期の菌の増殖を抑制するとともに，NK細胞あるいはγδ型T細胞からのIFN-γ産生を誘導する重要な役割を担っている．産生されたIFN-γはTNF-αとともにマクロファージを活性化し，殺菌活性の非常に強いNO産生を誘導して貪食した菌を殺菌処理する．また，このIFN-γは感染防御を司るT細胞の分化因子としても作用する．このように結核に対する初期防御反応では，感染局所で産生されたケモカインや炎症性サイトカインがマクロファージ，NK細胞やγδ型T細胞を感染部位に集め，それらを活性化し，その結果産生されたIFN-γがさらにマクロファージを活性化して，特異的防御免疫が成立するまでの期間，菌の増殖を最小限に抑えている．

2）獲得抵抗性の発現

結核菌を貪食したマクロファージやDCが産生するIL-12やIL-18，あるいはNK細胞やγδ型T細胞由来のIFN-γは，IFN-γ産生能を有する感染抵抗性Th1細胞を誘導する．このT細胞の分化誘導には，抗原提示細胞としてDCが重要な役割を果たしている．一方，結核菌はDCの機能を抑制することで感染宿主での生存を可能にすることが示されている[20]．Th1に分化したαβ型T細胞は，抗原およびIL-18の刺激を受けて大量のIFN-γを産生する．このため，感染防御を担うT細胞が出現するとマクロファージの殺菌能が飛躍的に高まる．感染免疫に関与するT細胞としては，クラスII拘束性$CD4^+$ Th1細胞ばかりではなく，クラスI拘束性$CD8^+$キラーT細胞も同時に誘導される．

ファゴソーム内で処理された細菌由来の抗原は通常クラスII分子に結合してT細胞に抗原提示されるため，$CD4^+$ Th1型T細胞により認識される．しかし，細胞質に存在する細菌由来抗原はプロテオソームにより消化されクラスI分子と会合するため，$CD8^+$ T細胞による認識を受ける．結核菌感染により誘導される$CD8^+$ T細胞は，$CD4^+$ T細胞と同様IFN-γを産生すると同時に，多量の菌を貪食して殺菌能の低下したマクロファージや菌が感染した非食細胞系細胞を破壊し，新たに動員されてくる活性化マクロファージに菌を処理させるという機構で感染防御に関与すると考えられる．また，$CD8^+$キラーT細胞は，結核菌感染細胞を傷害することで内部の菌を殺菌することができ，細胞質顆粒中に含まれるパーフォリンとグラニュリシンがこの殺菌メカニズムに関与することが報告されている[21]．さらに，タンパク質以外のLAM, PIM, glucose monomycolateやisoprenoid glycolipidなどの糖脂質成分がマクロファージ上のCD1分子に結合し，$CD8^+$あるいはダブルネガティブT細胞に抗原として提示されることがわかっている[22]．これらを認識するCD1拘束性T細胞は，抗原刺激後にIFN-γ産生やキラー活性を発揮することで防御免疫に関与することが示唆されている．また最近，IL-17産生性T細胞がCXCL9, CXCL10やCXCL11の産生を介して，感染局所へのIFN-γ産生性T細胞の動員に関与することが示された[23]．また，感染初期の肺ではIL-17産生性γδT細胞が結核に対する防御反応に関与することが示されている[24]．一方，制御性T細胞が結核感染で増加し，結核菌の排除の妨げになっていることも示されている[25]．このように，防御免疫の発現にはその機能あるいは認識する抗原が異なる多様なT細胞が関与する．感染の経過に伴いそれぞれのT細胞の防御免疫における比重は異なると考えられるが，これらT細胞活性の総和が結果的に結核菌に対する宿主の抵抗性を規定している．

おわりに

結核菌の病原性および宿主感染免疫のメカニズムについて，最近の知見を中心にまとめた．結核菌はヒトを宿主として共生することに成功した微生物であり，そのメカニズムが分子遺伝学的な手法で解析された結果，今までにみられなかった菌の感染動態や病原性の機序が明らかになってきた．今のところ，ヒトの免疫システムを回避する菌側のメカニズムは断片的にしか明らかになっていないが，それらは結核の病原機構を理解するうえでの最も重要な点であることは間違いない．これら研究成果の蓄積が新たな予防ワクチン開発の基礎となり，必ず結核菌の病原性の解明および結核の撲滅に結びつくものと期待される．